J. Cosmet. Sci., **63,** 333–344 (September/October 2012)

Preparation of emulsions by rotor–stator homogenizer and ultrasonic cavitation for the cosmeceutical industry

NG SOOK HAN, MAHIRAN BASRI, MOHD. BASYARUDDIN ABD. RAHMAN, RAJA NOOR ZALIHA RAJA ABD. RAHMAN, ABU BAKAR SALLEH, and ZAHARIAH ISMAIL, *Faculty of Science (N.S.H., M.B., M.B.A.R.), Institute of Bioscience (M.B., R.N.Z.R.A.R., A.B.S.), Faculty of Biotechnology and Biomolecular Sciences (R.N.Z.R.A.R., A.B.S.), Universiti Putra Malaysia, 43400 UPM Serdang, and Sime Darby Research Sdn Bhd, Carey Island, 42960 Pulau Carey (Z.I.), Selangor, Malaysia.*

Accepted for publication March 14, 2012.

Synopsis

Oil-in-water (O/W) nanoemulsions play an important key role in transporting bioactive compounds into a range of cosmeceutical products to the skin. Small droplet sizes have an inherent stability against creaming, sedimentation, flocculation, and coalescence. O/W emulsions varying in manufacturing process were prepared. The preparation and characterization of O/W nanoemulsions with average diameters of as low as 62.99 nm from palm oil esters were carried out. This was achieved using rotor–stator homogenizer and ultrasonic cavitation. Ultrasonic cell was utilized for the emulsification of palm oil esters and water in the presence of mixed surfactants, Tween 80 and Span 80 emulsions with a mean droplet size of 62.99 nm and zeta potential value at −37.8 mV. Results were comparable with emulsions prepared with rotor–stator homogenizer operated at 6000 rpm for 5 min. The stability of the emulsions was evaluated through rheology measurement properties. This included non-Newtonian viscosity, elastic modulus G', and loss modulus G''. A highly stable emulsion was prepared using ultrasonic cavitation comprising a very small particle size with higher zeta potential value and $G' > G''$ demonstrating gel-like behavior.

INTRODUCTION

An emulsion system consists of two immiscible liquids dispersed in one another and is thermodynamically unstable (1). An emulsion can be kinetically stable (long-term stability) with the presence of surfactant in the system by creating an energy barrier to flocculation and coalescence (2) and existing in a metastable state (3). Most emulsions fall into one of the two different classes: oil-in-water (O/W) and water-in-oil (W/O). The two types of emulsions are readily distinguished in principle, depending upon which kind of liquid forms the continuous phase (4). In O/W, tiny oil droplets

Address all correspondence to Mahiran Basri at mahiran@science.upm.edu.my.
Universiti Putra Malaysia, 43400 UPM Serdang, Selangor, Malaysia

are dispersed onto continuous phase, water. In W/O, water droplets are dispersed onto oil.

Palm oil esters were derived from palm oil and cis-9-octadecen-1-ol through enzymatic transesterification process using Lipozyme RM IM as the catalyst (5). The excellent wetting behavior of the esters without the oily feel make them have great potential in the manufacture of cosmeceutical products (6). The preparation of such emulsions with small droplet size is thus of particular interest. Small droplet sizes in general lead to greater emulsion stability (7). There are a number of mechanisms available for the production of such emulsions. The emulsification technique can be a form of mechanical mixing of two immiscible liquids where time is required for surfactant molecules to organize at the interface of the two phases.

Higher mechanical energy than what is possible from simple mixing can be achieved by rotor–stator systems. These systems are widely used to emulsify liquids of medium to high viscosity (7). The rotor–stator assembly consists of a rotor housed concentrically inside the stator with two or more blades and a stator with either vertical or slanted slots. As the rotor rotates, it generates a lower pressure to draw the liquid in and out of the assembly, resulting in circulation and emulsification (8). Ultrasound delivers even higher energy and is an alternative method of producing an emulsion. In ultrasound emulsification, the energy input is provided through sonotrodes (sonicator probe) containing a piezoelectric quartz crystal that can expand and contract in response to alternating electrical voltage.

Ultrasonic emulsification is believed to occur through two mechanisms. First, the application of an acoustic field produces interfacial waves that become unstable, eventually resulting in the eruption of the oil phase into the water medium in the form of droplets (9). Second, the application of low-frequency ultrasound causes acoustic cavitation, that is, the formation and subsequent collapse of microbubbles by the pressure fluctuations of a simple sound wave. Each bubble collapse event causes extreme levels of highly localized turbulence. The turbulent microimplosions act as a very effective method of breaking up primary droplets of dispersed oil into droplets of submicron size (10).

Work by Henglein and Gutierrez (11) indicated that at low-sonication amplitudes, the effect of the cavitation threshold was dominant and both the chemical yield and sonoluminescence arising from an acoustic field decreased with increasing pressure. Conversely, at higher amplitudes, the bubble collapse effects dominated and yields increased with increasing pressure. Similarly, Sauter *et al.* (12) found that low overpressures improve deagglomeration of nanoparticles, whereas higher overpressures had a negative effect.

Our study investigates the effect of different emulsification methods on the production of an O/W emulsion to produce an optimal droplet size for the production of the emulsion. The emulsions were also characterized using measurements of rheology properties, which were subsequently used to assess the physical stability of the emulsions, directly after preparation.

MATERIALS AND METHODS

MATERIALS

Emulsions were prepared with 15.8 wt% of palm oil esters (produced in our laboratory), 5 wt% of mixed surfactants, and 3 wt% tocotrienol (Gold Tri. E 70, purchased from Golden Hope Bioganic Sdn. Bhd, Selangor, Malaysia). Magnesium ascorbyl phosphate was purchased

from Spec-Chem Ind (Zhongshan, China). Butylated hydroxytoluene, xanthan gum, and beeswax were purchased from Fluka (St. Louis, USA). PEG-40 hydrogenated castor oil and phenonip were provided by Sime Darby Research Sdn. Bhd (Selangor, Malaysia). Deionized water was produced by using deionized water system (Milli-Q System; Massachusetts, USA). Two surfactants used were polyoxyethylene sorbitan monooleate (Tween 80) and sorbitan monooleate (Span 80), purchased from Sigma Aldrich (St. Louis, USA). Compositions of formulation are shown in Table I.

EMULSION PREPARATIONS

Rotor–stator method. The samples were produced by emulsification using hot–hot process. Emulsions were prepared where both oil and aqueous phases were separately warmed up to 70 ± 5°C. Xanthan gum was dispersed in deionized water at 0.8% w/w. Preparation of oil phase was performed by homogenizing 5% w/w of mixed Tween 80 and Span 80 (4:1) into oil phase of mixture with a Polytron homogenizer (Kinematica GmbH, Lucerne, Switzerland) rotor–stator. An emulsion sample of 100-ml total volume was prepared by pouring the oil phase into the aqueous phase and homogenizing at 6000 rpm for 5 min. The temperature was lowered to 40°C when the active ingredients and preservative were added. The emulsions were then subjected to mixing using stirrer (Ika-Werke, Staufen, Germany) at 200 rpm until reaching room temperature (25 ± 2°C) for 4 h.

Ultrasonic cavitation method. As a comparison, emulsions were also prepared using UP400S Hielscher Sonifier (Teltow, Germany) of 400 W nominal power and a frequency of 24 kHz equipped with a 22-mm sonotrode tip. This was placed in a custom-built cooling jacket. Chilled water at 3°C was continuously passed through this jacket. Emulsions were prepared where both oil and aqueous phases were separately warmed up to 70 ± 5°C. Xanthan gum was dispersed in deionized water at 0.8% w/w. An emulsion sample of 100-ml total volume was prepared and prehomogenized at 6000 rpm for 5 min with a Polytron homogenizer (Kinematica GmbH) rotor–stator. The temperature was lowered to 40°C. At 40°C, the active ingredients and preservative were added.

Table I
Chemical Compositions of Formulation Prepared By Rotor–Stator Homogenizer and Ultrasonic Cavitation

Ingredients	wt%	Function
External water phase (75°C ± 5°C)		
Water, deionized	63.70	Diluent/solvent
Xanthan gum	0.80	Thickener, emulsion stabilizer
Internal oil phase (75°C ± 5°C)		
Palm oil esters	15.80	Skin conditioning, emulsifier
PEG-40 hydrogenated castor oil	10.00	Surfactant/emulsifier
Beeswax	0.50	Skin conditioner
Polyoxyethylene sorbitan monooleate	4.00	Surfactant/emulsifier
Sorbitan monooleate	1.00	Surfactant/emulsifier
Active ingredients phase (40°C ± 5°C)		
Butylated hydroxytoluene	0.10	Lipophilic antioxidant
Tocotrienol	2.90	Vitamin E derivative—antioxidant
Magnesium ascorbyl phosphate	0.50	Vitamin C derivative—antioxidant
Phenonip	0.70	Preservatives

The emulsions were further homogenized using ultrasonic cavitation for 5 min. The sonifier tip horn was adjusted to 2 cm below the surface of a 100-ml sample. Sonication was performed at amplitude of 30 μm and 0.5 cycles.

PHYSICAL MEASUREMENTS

A Nanophox (Sympatec GmbH Instruments, Clausthal-Zellerfeld, Germany) was used to analyze the particle size distribution (PSD) of the finer emulsions formed. This device performs size measurements by photon cross-correlation spectroscopy, which measures the Brownian motion of colloidal particles, thus allowing the determination of their PSD. Samples were diluted with double-distilled water at one part of sample to two parts of water. The average drop size, expressed as the Sauter mean diameter ($d_{32} = \Sigma\, n_i d^3_i / \Sigma\, n_i d^2_i$, representing a surface average value), and the drop size distribution were obtained by means of a laser diffractometer according to the Mie theory. The Mie theory is a rigorous solution for the scattering intensity from a spherical, homogeneous, isotropic, and nonmagnetic particle of any diameter in a nonabsorbing medium. A refractive index of 1.460 was used for palm oil esters in Mie theory calculations. Emulsion particle size results are an average of six measurements of freshly prepared emulsions.

Zeta potential was measured using a Zetasizer Nano (Malvern Instruments, Worcestershire, UK). The samples were diluted (1:200) with distilled water and added into the equipment chamber. To obtain stable nanoemulsions (no flocculation and coalescence of the nanodroplets), zeta potential should usually reach a value of ±30 mV. The zeta potential results were obtained by applying the Henry equation:

$$U_E = \frac{2\varepsilon\zeta f\left(ka\right)}{3\eta} \tag{1}$$

where U_E is the electrophoretic mobility, ε is the dielectric constant, ζ is the zeta potential, η is the viscosity of the continuous phase, and $f(ka)$ is the Henry's function (13).

The rheology of O/W emulsions was characterized by using Kinexus Rotational Rheometer (Malvern Instruments, Worcestershire, UK). Two different rheological measurements were made to characterize the emulsions. First, viscosity versus shear stress, viscosity versus shear rate, and viscosity versus time plot at elevated temperature were applied to the emulsion samples. Second, oscillatory rheological measurements were made in the linear viscoelastic region, using 4°/40 mm cone and plate geometry and gap of 0.100 mm. All measurements were carried out at room temperature of 25.0 ± 0.5°C.

RESULTS AND DISCUSSION

SIZE DISTRIBUTION STUDIES

The size of an emulsion droplet formed by homogenization is controlled by the interplay between droplet breakup and droplet coalescence (14). Droplet breakup is controlled by the type and amount of shear applied to droplets, and the droplet resistance to deformation is determined by the surfactant. Droplet coalescence is determined by the ability of the surfactant to rapidly adsorb into the surface of newly formed droplets (14).

In the present study, Tween 80 and Span 80 were used as the mixed surfactants and the effect of PSD for emulsions prepared by rotor–stator emulsification and ultrasonic

cavitation is shown in Figure 1. The particle distribution for the two emulsions is expressed as a cumulative function. The resulting plots appear as double S-shaped curves. The particle size where the cumulative distribution is 50% is known as the median droplet diameter ($d_{v,0.5}$). The emulsion prepared by ultrasonic cavitation has a very small $d_{v,0.5}$ with 50% of the particles under 62.99 nm, compared to the emulsion prepared by rotor–stator emulsification, where the $d_{v,0.5}$ is 126.17 nm.

The relationship between emulsion particle size and emulsification systems can be explained in terms of energy input during emulsification. Emulsion droplet size (EDS) can be reduced by increasing the amount of energy supply during emulsification as long as there is sufficient emulsifier to cover new interface and recoalescence is prevented as much as possible (7). Conventionally, it would be expected that the amount of shear would increase with the applied energy and the emulsion particle size should then decrease with the increasing shear. The energy input required to produce an emulsion with a given EDS depends on the energy density of the emulsifying device. According to Canselier *et al.* (15), the Sauter mean diameter (d_{32}) can be calculated by involving the power density (P_V) and the residence time (t_{res}) in the emulsification zone:

$$d_{32} = {P_V}^{-b1}\, {t_{res}}^{-b2} \tag{2}$$

If both exponents are quite similar, and if two parameters are treated as a single variable, this equation represents the concept of "energy density" (16).

On the other hand, droplet disruption in rotor–stator systems is generally less efficient than ultrasonic devices because, according to Stang *et al.* (17), the dispersing zones of rotor–stator systems usually have larger volumes. Consequently, at constant energy density and volume flow rate, the mean power density in rotor–stator systems is lower and the mean residence time is longer than in ultrasonic devices. So, operating forces in a rotor–stator device act longer than the minimum time needed for droplet breakup. Therefore, emulsions prepared by using ultrasonic cavitation produced smaller droplet size.

ζ-POTENTIAL

Figure 2 shows that the ζ-potential values of emulsions prepared by rotor–stator and ultrasonic cavitation were −33.5 mV and −37.8 mV, respectively. An absolute value, less

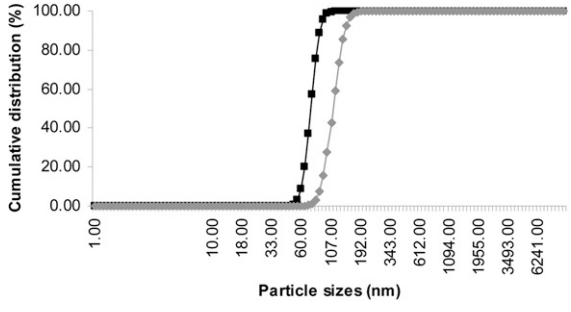

Figure 1. A comparison of emulsion particle distributions obtained for 30% w/w palm oil esters-in-water emulsions stabilized by 5% w/w mixed surfactants, Tween 80 and Span 80, which were prepared using rotor–stator homogenizer (—◆—) and ultrasonic cavitation (—■—).

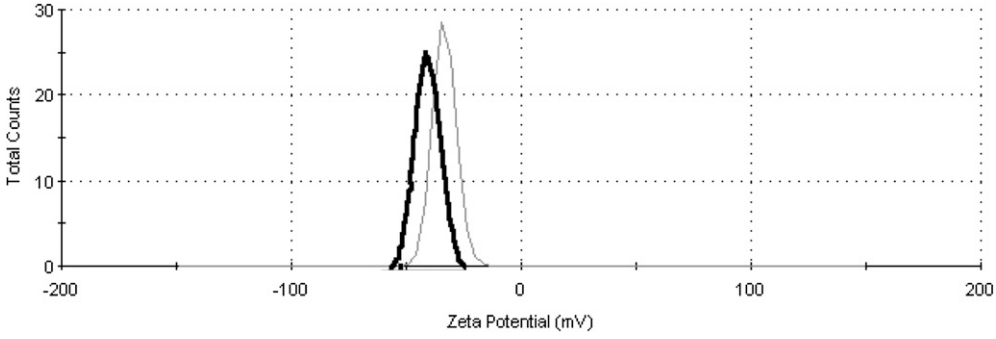

Figure 2. The zeta potential of emulsions measure for emulsion prepared by using rotor–stator homogenizer (——) and ultrasonic cavitation (——).

than or greater than 25 mV is indicative of flocculated and deflocculated emulsions, respectively (18). Therefore, no flocculation was shown in both emulsions. The results indicated that the droplet stability in the emulsions prepared by ultrasonic cavitation was higher than the emulsions prepared by rotor–stator. This could be due to the increase in energy input during emulsification. The higher the absolute value of zeta potential, the larger the electrostatic repulsive forces and the separation of the particles become easier.

According to the DLVO (Derjaguin–Landau–Verwey–Overbeek) theory, a system can be regarded as stable if the electrostatic repulsion dominates the attractive van der Waals force (19). The particles have to overcome an energy barrier of electrostatic repulsion to approach closely and form agglomerates. Smaller droplet size provides an enhanced kinetic stability in the inner droplets to coalescence or agglomerate in addition to lowered interfacial tension. It was observed that the EDS prepared by ultrasonic cavitation were smaller than the EDS prepared by rotor–stator emulsification. The very small droplet size caused a large reduction in the gravity force, and the Brownian motion may be sufficient in overcoming gravity. Thus, no creaming or sedimentation could occur and the electrostatic repulsion dominates the attractive van der Waals force.

RHEOLOGICAL CHARACTERIZATION 1: VISCOSITY VERSUS SHEAR RATE PLOT

Figure 3 shows a log/log plot on the effect of increasing energy input on the functional relationship between viscosity and shear rate for emulsions. A drastic decrease in the viscosity of these emulsions was observed. The viscosity of 109.69 Pa·s for emulsion prepared by rotor–stator emulsification decreased to 70.79 Pa·s after sonication for 5 min. The interactions between the emulsion molecules will be weakened and, as a result, the viscosity would be decreased by the destruction of the network. It was clearly indicated that the differences in the changes in viscosity were not very large, but still significant. The linear portions of the plots are readily fitted to the Power Law model shown in equation (3):

$$\eta = k\dot{\gamma}^{n-1} \tag{3}$$

where η is the viscosity (Pa·s^{-1}), $\dot{\gamma}$ is the strain rate (s^{-1}), k is the consistency index of the emulsion, and n is the power (shear thinning) index ($n < 1$). Decreasing the value of n increased the degree of shear thinning of the emulsion system.

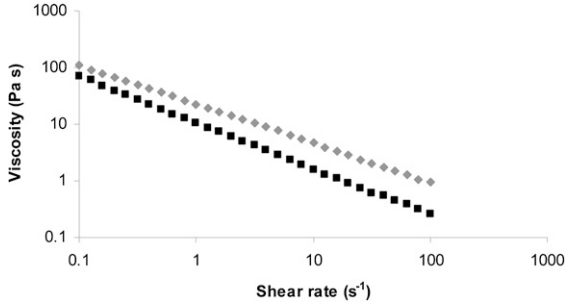

Figure 3. Rheological characterization of 30% w/w palm oil esters-in-water emulsions prepared using rotor–stator homogenizer (◆) and ultrasonic cavitation (■).

The degree of pseudoplasticity can also be indicated by the power index (n), which decreases when pseudoplasticity increases. The applicability of the Power Law model exhibited n values ranging between 0.14 (for emulsions prepared with ultrasonic cavitation) and 0.18 (for emulsions prepared with rotor–stator homogenizer) with the regression coefficients (r^2) ranging between 0.9912 and 0.9973 (Table II). The emulsion prepared with ultrasonic cavitation was found to be more pseudoplastic with the lowest flow index. In terms of the consistency coefficient (k), the emulsions prepared with ultrasonic cavitation showed the higher consistency. The consistency is an indicator of the viscous nature of the emulsion.

At high shear rates, there is some discernible departure from linearity, with the curvature suggesting the attainment of a constant viscosity at high shear rates. Such behavior is expected for shear-thinning systems. Shear-thinning behavior in emulsions can be interpreted as indicating the presence of weak attractive forces between the emulsion droplets, which give rise to the formation of a weak elastic gel-like network (20). The dependence of the viscosity on the shear rate indicated that the emulsions were typical non-Newtonian in behavior.

RHEOLOGICAL CHARACTERIZATION 2: SHEAR STRESS VERSUS SHEAR RATE PLOT

Figure 4 is a log/log plot indicating how increasing energy input affects the functional relationship between shear stress and shear rate. It also shows that the data can be adequately fitted to the Herschel–Bulkeley model. The Herschel–Bulkeley model takes the form (21):

$$\tau = \tau_0 + k_{HB}\dot{\gamma}^{\alpha} \tag{4}$$

Table II
Power Law Parameters Obtained From the Data Shown in Figure 3 Fitting to the Power Law Equation

Emulsification	n	k	r^2
Rotor–stator	0.18	10.6	0.9973
Ultrasonic	0.1378	13.84	0.9912

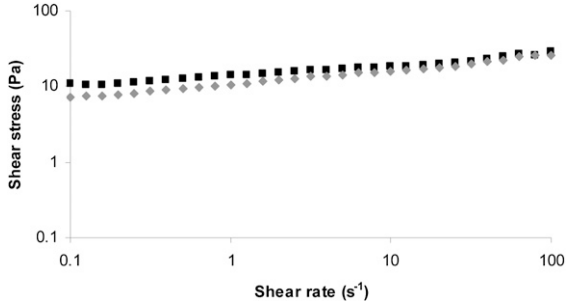

Figure 4. A plot of shear stress as a function of shear rate for 30% w/w palm oil esters-in-water emulsions prepared using rotor–stator homogenizer (◆) and ultrasonic cavitation (■).

where τ is the shear stress (Pa), τ_0 is the apparent yield stress, $\dot{\gamma}$ is the shear rate (s^{-1}), and k_{HB} and α are model constants. The model accounts for the fact that for any system that possess a network structure, the initial application of shear results in distortion of the network. Once the applied stress is greater than the yield stress, non-Newtonian flow will occur. The apparent yield stress values for the emulsions were obtained from the fitting process and are shown in Table III.

The attractive force is one of the colloidal interactions and plays an important role in the increase in yield stress. This is because the magnitude of yield stress depends on the strength of the attractive force between the droplets (22). The decrease of droplet size resulting from the increase in the disperse phase volume fraction causes an increase in the total droplet surface area. When the total droplet surface area increases, the strength of the attractive force increases accordingly. Thus, greater stress is required to initiate flow when a high attractive force is holding the droplets resulting in high yield stress (22). A very low yield stress may indicate a tendency to separation.

RHEOLOGICAL CHARACTERIZATION 3: FREQUENCY DEPENDENCE OF DYNAMIC MODULI

The viscous and elastic responses of viscoelastic systems can be quantified by dynamic oscillatory measurements. Profiles showing frequency dependence of dynamic moduli for emulsions prepared with rotor–stator homogenizer and ultrasonic cavitation are given in Figures 5 and 6, respectively. The data show how the storage modulus, G' and loss modulus, G'' change as a function of frequency. These ω dependence of dynamic moduli suggest that G' response of these samples is dominant over G'' response throughout the entire measured ω domain, implying that solid-like (elastic) property dominates over liquid-like (viscous) property in these emulsion samples. This indicates the presence of a

Table III
Herschel–Bulkeley Parameter Obtained From the Data Shown in Figure 4

Emulsification	Yield stress (Pa)
Rotor–stator	7.29
Ultrasonic	10.98

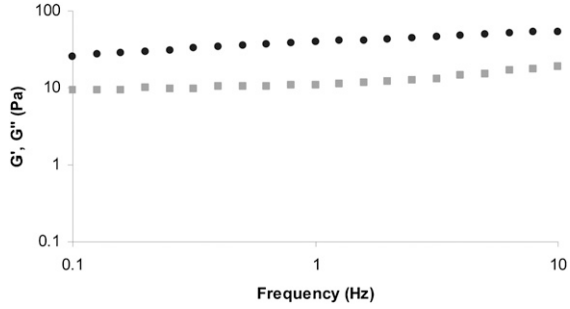

Figure 5. A frequency sweep of an emulsion system that shows an elastic response to shear. The diagram shows the storage (G'; ●) and loss (G''; ■) moduli for an emulsion system prepared by rotor–stator homogenizer.

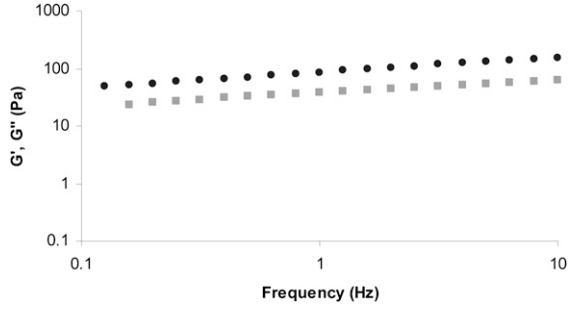

Figure 6. A frequency sweep of an emulsion system that shows an elastic response to shear. The diagram shows the storage (G'; ●) and loss (G''; ■) moduli for an emulsion system prepared by ultrasonic cavitation.

network structure created between dispersed phase droplets. The practical implication of this behavior is that emulsions show high stability and longer storage life if they exhibit domination of G' response over G'' (23).

In point of emulsification methods, emulsions prepared using ultrasonic cavitation exhibited better viscoelastic responses when compared to those prepared by rotor–stator homogenizer. The fact that the G' response of emulsions prepared by ultrasonic cavitation was higher than the response of emulsions prepared by rotor–stator homogenizer is evidence that the degree of elastic property of emulsions prepared by ultrasonic cavitation is higher. This in turn suggests that emulsions prepared by ultrasonic cavitation are more stable and possess longer shelf life compared to emulsions prepared by rotor–stator homogenizer. As G'' response of emulsions prepared by ultrasonic cavitation was higher compared to emulsions prepared by rotor–stator homogenizer at all measured frequency domains, it is evident that the emulsions prepared by ultrasonic cavitation systems flow and spread more easily compared to corresponding emulsions prepared by rotor–stator homogenizer system.

Plot of phase angle δ as a function of frequency ω is given in Figures 7 and 8. In Figure 7, the phase angle is less than 20° across the entire frequency range, indicating that the system tends to show an elastic response to shear. On the other hand in Figure 8, the phase angle at low frequency shows that the response of the system is elastic. As the frequency increases, the response of the system becomes more viscous. Such behavior is a common feature in viscoelastic systems.

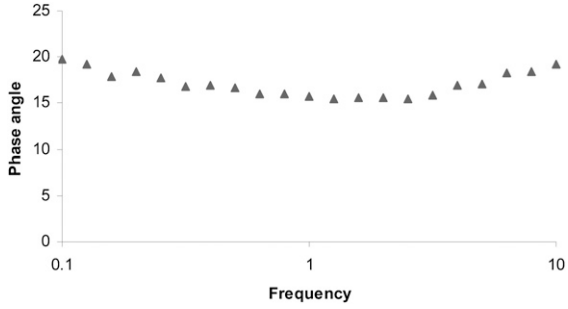

Figure 7. A phase angle graph shows how the phase angle varies with frequency for emulsion system prepared by rotor–stator homogenizer.

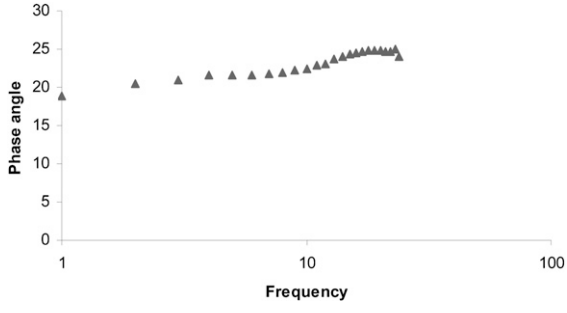

Figure 8. A phase angle graph shows how the phase angle varies with frequency for emulsion system prepared by ultrasonic cavitation.

RHEOLOGICAL CHARACTERIZATION 4: TIME-DEPENDENT VISCOMETRY

Time-dependent viscometry was used to explore the consequences of structural changes during floc development. Emulsions were initially sheared at high stress (10 Pa) to breakup any existing flocs. After 1 min, this stress was removed and a constant low shear stress (0.1 Pa) was applied for 300 s where viscosity measurements taken every 1 s with increasing temperature in the range from 25°C to 50°C. Figures 9 and 10 show the apparent viscosity versus time plot at elevated temperature for the stabilized emulsion prepared by rotor–stator emulsification and ultrasonic cavitation, respectively.

After the applied stress was removed, an immediate increase in apparent viscosity was observed, which could be attributed to the onset of flocculation. The apparent viscosity was found to reach a maximum of 109.69 Pa·s and 70.79 Pa·s at 25°C, after which it was followed by a steady decrease to 108.50 Pa·s and 70.09 Pa·s over the remaining time (300 s) for emulsions prepared by rotor–stator and ultrasonic cavitation, respectively. It can be seen that there was no change in emulsion viscosity over the time at elevated temperatures, as would be expected for an emulsion not displaying time-dependent flocculation.

CONCLUSION

The ultrasonic cavitation as compared to rotor–stator is a viable method for producing nanoemulsions of palm oil esters in water with mean particle sizes down to 62.99 nm and

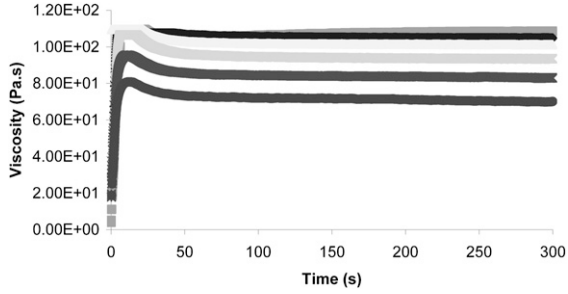

Figure 9. Time-dependent apparent viscosity at 25°C (■), 30°C (◆), 35°C (▲), 40°C (×), 45°C (✱), and 50°C (●) for an emulsion system prepared by rotor–stator homogenizer.

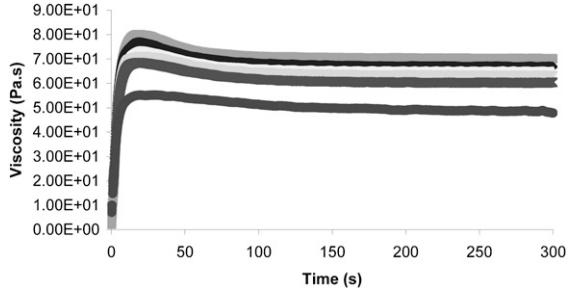

Figure 10. Time-dependent apparent viscosity at 25°C (■), 30°C (◆), 35°C (▲), 40°C (×), 45°C (✱), and 50°C (●) for an emulsion system prepared by ultrasonic cavitation.

zeta potential of −37.8 mV after 5 min of sonication. Physically stable O/W emulsions were prepared using ultrasonic cavitation and rotor–stator homogenizer, where $G' > G''$ and the emulsion displays gel-like properties. Under appropriate conditions, the emulsions develop an elastic network that provides the emulsions with good long-term stability to coalescence.

ACKNOWLEDGMENT

The authors thank Universiti Putra Malaysia for the financial support given for this project.

REFERENCES

(1) P. Somasundaran, T. H. Wines, S. C. Metha, N. Garti, and R. Farinato, *Emulsions and Their Behavior in Surfactants in Personal Care Products and Decorative Cosmetics* (CRC Press, Boca Raton, New York, 2007), p. 504.
(2) D. L. Marshall and L. B. Bullerman, *Antimicrobial Properties of Sucrose Fatty Acid Esters in Carbohydrate Polyesters as Fat Substitutes* (Marcel Dekker, New York, 1994).
(3) D. J. McClements, *General Characteristics of Food Emulsions in Food Emulsions: Principles, Practice and Techniques* (CRC Press, Boca Raton, New York, 1999), p. 2.
(4) L. L. Schramm, *In Emulsions, Foams, Suspension: Fundamental and Application* (Wiley VCH Verlag GmbH & Co, Germany, 2006), pp. 1–260.

(5) P. S. Keng, M. Basri, M. B. Abdul Rahman, M. R. S. Zakaria, A. B. Ariff, R. N. Z. Abdul Rahman, and M. B. Salleh, Newly synthesized palm esters for cosmetic industry, *J. Ind. Crops Prod.,* **29,** 37–44 (2008).
(6) E. R. Gunawan, M. Basri, M. B. Abdul Rahman, A. B. Salleh, and R. N. Z. Abdul Rahman, Study on response surface methodology (RSM) of lipase-catalyzed synthesis of palm-based wax esters, *Enzyme Microb. Technol.,* **37,** 739–744 (2005).
(7) D. J. McClements, *Food Emulsions: Principles, Practices and Technique, 2nd Ed.* (CRC Press, Boca Raton, New York, 2005).
(8) Y. F. Maa and C. C. Hsu, Liquid-liquid emulsification by rotor/stator homogenization, *J. Controlled Release,* **38,** 219–228 (1996).
(9) M. K. Li and H. S. Fogler, Acoustic emulsification. Part 1. The instability of the oil-water interface to form the initial droplets, *J. Fluid Mech.,* **88** (3), 499–511 (1978).
(10) M. K. Li and H. S. Fogler, Acoustic emulsification. Part 2. Break-up of the larger primary oil droplets in a water medium, *J. Fluid Mech.,* **88** (3), 513–528 (1978).
(11) A. Henglein and M. Gutierrez, Sonochemistry and sonoluminescence: Effects of external pressure, *J. Phys. Chem.,* **97,** 158–162 (1993).
(12) C. Sauter, M. A. Emin, H. P. Schuchmann, and S. Tavman, Influence of hydrostatic pressure and sound amplitude on the ultrasound induced dispersion and de-agglomeration of nano-particles, *Ultrason. Sonochem.,* **15,** 517–523 (2008).
(13) H. Mirhosseini, C. P. Tan, N. S. A. Hamid, and S. Yusof, Effect of Arabic gum, xanthan gum and orange oil contents on zeta potential, conductivity, stability, size index and pH of orange beverage emulsion, *Colloids Surf., A,* **315,** 47–56 (2008).
(14) T. Tadros, P. Izquierdo, J. Esquena, and C. Solans, Formation and stability of nano-emulsions, *Adv. Colloid Interface Sci.,* **108–109, 303–318** (2004).
(15) J. R. Canselier, H. Delmas, A. M. Wilhelm, and B. Abismail, Ultrasound emulsification—An overview, *J. Dispersion Sci. Technol.,* **23,** 333–349 (2002).
(16) B. Abismail, J. P. Canseliar, A. M. Wilhelm, H. Delmas, and C. Gourdon, Emulsification processes: On-line study by multiple light scattering measurements, *Ultrason. Sonochem.,* **7,** 187–192 (2000).
(17) M. Stang, H. Schuchmann, and H. Schubert, Emulsification in high-pressure homogenizers, *Eng. Life Sci.,* **1,** 151–157 (2001).
(18) H. A. Leiberman, M. M. Reiger, and G. S. Banker, *Pharmaceutical Dosage Forms: Disperse Systems* (Marcel Dekker, New York, 1989), Vol. 2.
(19) A. Grabbe and R. G. Horn, Double-layer and hydration forces measured between silica sheets subjected to various surface treatments, *J. Colloid Interface Sci.,* **157,** 375–383 (1993).
(20) E. Dickinson, *An Introduction of Food Colloids* (Oxford University Press, Oxford, 1992).
(21) J. H. Prentice, *Measurements in the Rheology of Foodstuffs* (Elsevier Applied Science Publishers, London, 1984).
(22) R. Pal, *Rheology of Emulsions Containing Polymeric Liquids: Encyclopedia of Emulsion Technology* (Marcel Dekker, New York, 1996).
(23) B. B. Niraula, N. S. Tiong, and M. Misran, Vesicles in fatty acid salt—fatty acid stabilized o/w emulsion—emulsion structure and rheology, *Colloids Surf., A,* **236,** 7–22 (2004).